Stochastic Differential Equation-Based Mixed Effects Model of the Fluid Volume in the Fasted Stomach in Healthy Adult Human

Kai Wang[1], Luca Marciani[2], Gordon L. Amidon[1], David E. Smith[1], and Duxin Sun[1]
1 Department of Pharmaceutical Sciences, University of Michigan, Ann Arbor, Michigan 48109, United States
2 Nottingham Digestive Diseases Centre and National Institute for Health Research (NIHR) Nottingham Biomedical Research Centre, Nottingham University Hospitals NHS Trust and University of Nottingham, United Kingdom
- Corresponding author: Kai Wang, kaiwangy@umich.edu, +1 7347809605

Key words
Stochastic differential equation; gastric emptying; oral absorption; population model; Extended Kalman Filter

Abstract
The rate and extent of drug dissolution and absorption from a solid oral dosage form depend largely on the fluid volume along the gastrointestinal tract. Hence a model built upon the gastric fluid volume profiles can help to predict drug dissolution and subsequent absorption. To capture the great inter- and intra-individual variability (IAV) of the gastric fluid volume in fasted human, a stochastic differential equation (SDE)-based mixed effects model was developed and compared with the ordinary differential equation (ODE)-based model. Twelve fasted healthy adult subjects were enrolled and had their gastric fluid volume measured before and after consumption of 240 mL of water at pre-determined intervals for up to 2 hours post ingestion. The SDE- and ODE-based mixed effects models were implemented and compared using Extended Kalman Filter algorithm via NONMEM. The SDE approach greatly improved the goodness of fit compared with the ODE counterpart. The proportional and additive measurement error of the final SDE model decreased from 14.4% to 4.10% and from 17.6 mL to 4.74 mL, respectively. The SDE-based mixed effects model successfully characterized the gastric volume profiles in the fasted healthy subjects, and provided a robust approximation of the physiological parameters in the very dynamic system. The remarkable IAV could be further separated into system dynamics terms and measurement error terms in the SDE model instead of only empirically attributing IAV to measurement errors in the traditional ODE method. The system dynamics were best captured by the random fluctuations of gastric emptying coefficient Kge.

Introduction
The hydrodynamics in the gut is one of the determining factors for oral drug absorption. Firstly, the transit rate of drugs carried by luminal fluid flow directly affects the rate of drug systemic appearance. Specifically, for the Biopharmaceutics Classification System (BCS) Class 1 drugs, transit with the fluid flow driven by gastrointestinal (GI) motility is the only physiological source of intra-individual variability (IAV) in the systemic appearance profiles. Secondly, the impact of dissolution in GI fluid on oral absorption is prominent for drug substances with low aqueous solubility. As we know, being dissolved in gut fluid is a prerequisite for solid drug oral absorption, so the impact of dissolution is greatly amplified in the case of poorly aqueous soluble drugs exposed to variable gut luminal fluid volume, potentially as well as fluctuating fluid pH if they are

ionizable. In other words, the fluid dynamics plus the varying luminal pH in the gut may regulate the rate and the extent of oral absorption for these drugs.

As the starting point of diving into the fluid dynamics of the gut, the fluid volume profiles in the fasted stomach among healthy adult subjects is essential yet difficult to fully characterize. Since the change in the volume of the fasted stomach is a function of saliva and gastric secretion, gastric emptying (GE), and oral intake of water, a model built upon the observed gastric fluid volume at given sampling times can be used to describe these important GI physiological process under interdigestive conditions. This is the basis for a more mechanistic approach to predicting drug disintegration, dissolution, and subsequent systemic appearance profiles. The predictive results are particularly important for the monitoring of highly variable drugs with narrow therapeutic windows and the design of bioequivalence (BE) studies. Conventionally, GE was described as a first-order process with time-invariant parameters and the gastric fluid volume was not considered explicitly, but a growing amount of research has demonstrated that GI events are very dynamic[1]. The half-time of GE varied from 8 to 18 minutes and relied heavily on the phases of the fasting conditions divided by cyclical migrating motor complex (MMC) [2-6]. It was also reported by Mudie et al that 25% of the subjects displayed non-first order GE pattern[7]. In addition, gastric secretion increases to its peak at early Phase 3 of MMC from the nadir at Phase 1[8, 9].

Stochastic differential equation (SDE)-based mixed effects model is preferred in the intrinsically non-deterministic system to provide robust parameter estimation, and to serve as a diagnostic tool for structural model misspecification or parameter fluctuations. In contrast to the classical ordinary differential equation (ODE)-based population approach, where IAV is only assigned to measurement errors, the employment of SDE method allows for separation of the IAV into a system noise term arising from time-dependent or serial correlated errors like unknown or incorrectly specified dynamics, and a measurement noise term accounting for uncorrelated errors such as assay error[10].

This study is aimed: (1) to capture the great inter-individual variability (IIV) and IAV of the fluid dynamics in the fasted stomach among healthy adult subjects; (2) to determine the physiological parameter(s) representing the dynamics in the stomach by implementing the SDE method and comparing the results with ODE.

Materials and Methods

Study design

Twelve fasted healthy adult subjects were enrolled and had their gastric and small intestinal water volume measured by magnetic resonance imaging scans before and after consumption of 240 mL of water at pre-determined intervals for up to 2 hours post ingestion[7].

Model assumption

The fluid volume in the stomach compartment was basically modeled with a bolus input of 240 mL water defined by the input function D, zero-order saliva and gastric secretion with the coefficient Kse, and first-order GE with the coefficient Kge. This structural model was shared across all the tested models in this study and the corresponding equation was included in Equation (1).

The IAV of gastric fluid volume was assumed as a combination of system dynamics arising from the fluctuations of pharmacokinetic (PK) parameter(s) and measurement errors. The possible fluctuations of PK parameters were checked in the scenario of: (1) time-invariant Kse and time-invariant Kge, (2) time-varying Kse and time-invariant Kge, (3) time-invariant Kse and time-varying Kge (shown as an example in Equation (1) and depicted in Fig. 1), and (4) time-varying Kse and time-varying Kge, by Ornstein-Uhlenbeck process, respectively. Both the homoscedasticity and heteroscedasticity of the measurement errors were considered in Equation (2).

For subject i at j^{th} sampling time:

Continuous time state space stochastic differential equations:

$$d\begin{pmatrix}\mathrm{Xstomach_i}\\ \mathrm{logKge_i}\end{pmatrix}=\begin{pmatrix}-\mathrm{Kge_i}\times\mathrm{Xstomach_i}+\mathrm{Kse_i}+\mathrm{D(t)}\\ -\alpha_{\mathrm{Kge}}(\mathrm{logKge_i}-\mathrm{logKge_i^*})\end{pmatrix}dt+\begin{pmatrix}0 & 0\\ 0 & \sigma_{\mathrm{wKge}}\end{pmatrix}dW_i(t),$$

$$W_{it}-W_{is}\in N(0,|t-s|I),\ D(t)=\begin{cases}240\ \mathrm{mL},\ t=0\\ 0,\ \mathrm{otherwise}\end{cases} \quad (1)$$

Discrete time measurement equations:

$$\mathrm{Ystomach_{ij}}=\mathrm{Xstomach_{ij}}\times\left(1+\sigma_{\mathrm{prop}}\varepsilon_{1ij}\right)+\sigma_{\mathrm{add}}\varepsilon_{2ij},\begin{pmatrix}\varepsilon_{1ij}\\ \varepsilon_{2ij}\end{pmatrix}\sim N\left(\begin{pmatrix}0\\ 0\end{pmatrix},\begin{pmatrix}1 & 0\\ 0 & 1\end{pmatrix}\right) \quad (2)$$

where $\mathrm{Xstomach_i}$ is the gastric fluid volume state variable, $\mathrm{Ystomach_{ij}}$ is the gastric fluid volume observation variable, D is the input function of water, $\mathrm{Kse_i}$ is the constant saliva and gastric secretion coefficient, $\mathrm{Kge_i}$ is the time-varying GE coefficient, $\mathrm{logKge_i}$ is the logarithm of $\mathrm{Kge_i}$, $\mathrm{logKge_i^*}$ is the constant typical individual mean of $\mathrm{logKge_i}$, α_{Kge} denotes the mean reversion speed of Kge, σ_{wKge} is the scaling diffusion term, I is the identity matrix, W(t) is a standard Weiner process also referred to as Brownian motion. The standard Weiner process is a stochastic process with mutually independent increments (W_t - W_s) from time t to s which are Gaussian distributed with mean zero and variance |t – s|I. ε_1 and ε_2 are two mutually independent standard normal distributions with mean 0 and variance 1. σ_{prop} and σ_{add} are the scaling term of the proportional and additive measurement errors, respectively.

The fluctuation of $\mathrm{Kge_i}$ refers to the deviation of the time-varying Kge of subject i at certain time t ($\mathrm{Kge_i(t)}$) from its constant typical individual mean value $\mathrm{Kge_i^*}$. The nonnegativity of $\mathrm{Kge_i(t)}$ is ensured by using the logarithm form in this Ornstein-Uhlenbeck diffusion process. $\sigma_{\mathrm{wKge}}dW_i(t)$ drives the fluctuations of $\mathrm{logKge_i}$, which follows a Weiner process. The component $-\alpha_{\mathrm{Kge}}(\mathrm{logKge_i} - \mathrm{logKge_i^*})$ acts like a negative feedback mechanism, and keeps the fluctuations of $\mathrm{logKge_i}$ at a proper range away from $\mathrm{logKge_i^*}$. If the diffusion term σ_{wKge} is zero, the SDE model reduces to the ODE model. The physiological interpretation of the dynamic parameters is thereby preserved in the SDE model formulation.[11]

The IIV of PK parameters were described in the same way for SDE models as for the ODE model in Equation (3) and Equation (4). The typical individual parameters were modeled as a function of the fixed-effects population parameters and random-effects parameters.

For subject i:

Inter-individual variability:

$$\mathrm{Kge_i^*}=\mathrm{Kge^*}\times\exp\left(\eta^*_{\mathrm{Kgei}}\right),\eta^*_{\mathrm{Kgei}}\sim N(0,\omega^2_{\mathrm{Kge}}) \quad (3)$$

$$\mathrm{Kse_i}=\mathrm{Kse}\times\exp(\eta_{\mathrm{Ksei}}),\eta_{\mathrm{Ksei}}\sim N(0,\omega^2_{\mathrm{Kse}}) \quad (4)$$

where Kge_i^* and Kse_i are the constant typical individual mean of GE coefficient and saliva and gastric secretion coefficient, respectively. Accordingly, Kge^* and Kse are the population means. The corresponding random-effects parameters η_{Kgei}^* and η_{Ksei} are mutually independent normally distributed with zero mean and standard deviation ω_{Kge} and ω_{Kse}. The three levels of random effects, IIV, parameter fluctuations and measurement errors were mutually independent for all t, j, and i.

The SDE- and ODE-based mixed effects models were implemented and compared using Extended Kalman Filter (EKF) algorithm and first-order conditional estimation (FOCE) method in NONMEM.

Algorithm

The recursive EKF consists of the prediction equations and the update equations. The prediction equations predict the state and output variables one step ahead, that is, from the previous measuring time until the current measuring time. The update equations update the state predictions with the observed data collected at the current measuring time. The updated state predictions are then used as the initial conditions for the prediction equations starting from the current measuring time until the next measuring time.[11] The Extended Kalman Filter (EKF) is implemented to estimate state variables on individual level. In the case of the SDE with time-varying Kge model, for subject i at j^{th} measurement, the state variables were $Xstomach_i$ and $logKge_i$, and the output variable was $Ystomach_{ij}$. The corresponding equations are written out as follows.

Step 1: one-step state prediction

The optimal (minimum variance) prediction of the means and covariances of the state variables for subject i at j^{th} measurement, can be calculated by solving the state ($\widehat{X}_{i(t|j-1)}$) and state covariance ($\widehat{P}_{i(t|j-1)}$) equations from measuring time t_{j-1} until t_j, that is,

$$\frac{d\widehat{X}_{i(t|j-1)}}{dt} = g(\widehat{X}_{i(t|j-1)}, D(t)_i, \phi_i) \quad (5)$$

$$\frac{d\widehat{P}_{i(t|j-1)}}{dt} = A_{it}P_{i(t|j-1)} + P_{i(t|j-1)}A_{it}^T + \sigma_w\sigma_w^T, \quad A_{it} = \frac{\partial g}{\partial x}|_{x=\hat{x}_{i(t|j-1)}}, \quad t \in [t_{j-1}, t_j] \quad (6)$$

where ϕ_i is the individual parameter vector.

Step 2: one-step output prediction

$$\widehat{Y}_{i(j|j-1)} = E\left[Y_{ij}|Y_{i(j-1)}, \dots, Y_{i1}\right] = f(\widehat{X}_{i(j|j-1)}) \quad (7)$$

$$R_{i(j|j-1)} = Var\left[Y_{ij}\middle|Y_{i(j-1)}, \dots, Y_{i1}\right] = C_{ij}P_{i(j|j-1)}C_{ij}^T + \Sigma, \quad C_{ij} = \frac{\partial f}{\partial x}|_{x=\hat{x}_{i(j|j-1)}} \quad (8)$$

The one-step output prediction $\widehat{Y}_{i(j|j-1)}$ is the optimal prediction of the j^{th} measurement before that measurement is taken ($\widehat{X}stomach_{i(j|j-1)}$ in this case), while $R_{i(j|j-1)}$ is the expected covariance for that prediction. $R_{i(j|j-1)}$ is thus the sum of the state covariance associated with the observed states ($C_{ij}P_{i(j|j-1)}C_{ij}^T$) and measurement covariance (Σ).

Step 3: state update

The one-step state and state covariance predictions are updated by conditioning on the j^{th} measurement using the EKF state update equations, that is,

$$K_{ij} = P_{i|j-1} C_{ij}^{T} R_{i(j|j-1)}^{-1} \quad (9)$$

$$\widehat{X}_{i(j|j)} = \widehat{X}_{i(j|j-1)} + K_{ij}(Y_{ij} - \widehat{Y}_{i(j|j-1)}) \quad (10)$$

$$P_{i(j|j)} = P_{i(j|j-1)} - K_{ij} R_{i(j|j-1)} K_{ij}^{T} \quad (11)$$

where $\widehat{X}_{i(j|j)}$ is the updated state estimate, $P_{i(j|j)}$ is the updated state covariance, and K_{ij} is called the Kalman gain. The optimal state estimate $\widehat{X}_{i(j|j)}$ is equal to the best state prediction before the measurement is taken $\widehat{X}_{i(j|j-1)}$ plus a correction term consisting of an optimal weighting value times the difference between the measurement Y_{ij} and the one-step prediction of its value.[11]

Results

Raw data visualization

There exists great IIV and IAV in the observed gastric volume data in Fig. 2, indicating it is very necessary to develop a hierarchical and SDE-based model to capture the variabilities, respectively.

Model Selection

The three SDE models in Table 1 showed significant improvement in goodness of fit compared with the traditional ODE model. The parsimonious model with the lowest objective function value, that is SDE with time-varying Kge model, was considered to best characterize the gastric fluid volume profiles and was chosen for further analysis. This finding implied that the fluctuations of gastric emptying coefficient Kge might be the driving factor for the system dynamics of gastric fluid volume.

Table 1 A brief description of the tested models

Models	Objective function value	Diffusion process
ODE	1406.405	$\alpha = 0$ and $\sigma_w = 0$
SDE with time-varying Kse	1284.873	$dlogKse_i = -\alpha_{Kse}(logKse_i - logKse_i^{*})dt + \sigma_{wKse}dW_i(t)$
SDE with time-varying Kge	1214.567	$dlogKge_i = -\alpha_{Kge}(logKge_i - logKge_i^{*})dt + \sigma_{wKge}dW_i(t)$
SDE with time-varying Kse and Kge	1214.567	$dlogKse_i = -\alpha_{Kse}(logKse_i - logKse_i^{*})dt + \sigma_{wKse}dW_i(t)$ and $dlogKge_i = -\alpha_{Kge}(logKge_i - logKge_i^{*})dt + \sigma_{wKge}dW_i(t)$

ODE: ordinary differential equation; SDE: stochastic differential equation

Final model results

The estimates of the typical population mean of Kge and Kse all fell into the physiological ranges reported in the literatures in both the SDE with time-varying Kge model and the ODE model. The proportional and additive measurement error were decreased from 14.4% to 4.10% and from 17.6 mL to 4.74 mL for the fluid volume in the stomach compartment by SDE compared with ODE, respectively. This indicated that a large part of IAV arose from the system dynamics especially the fluctuations of Kge. These serial correlated errors would be ignored and empirically assigned to the measurement errors if we adopted the traditional ODE method. The relative standard errors (RSE) were similar in the SDE and ODE models.

The time-varying nature of Kge was numerically and graphically shown in Table 2 and Fig. 3 compared with the constant estimates in ODE for each individual in this study, and was considered as the major source of the dynamics in the gastric fluid volume system.

The one-step individual SDE predictions, updates, and prediction interval were shown together with the individual ODE predictions in Fig. 4. The observed discrepancy between the SDE and ODE predictions could be explained by the SDE predictions being conditioned on all previous observations and updated at each sampling time, which was visualized as the vertical lines in the SDE predictions.

Table 2 Parameter Estimation of the SDE with time-varying Kge model and the ODE model

Model		**SDE**		**ODE**	
Parameters		Estimates	RSE(%)	Estimates	RSE(%)
Physiological	Kge (/min)	0.0514	17.6	0.0714	9.02
	Kse (mL/min)	1.52	13.4	1.59	13.9
Intra-individual variability	$\sigma_{wkge}(min^{-1/2})$	0.251	9.42	0	na
	α_{kge}(/min)	0.0204	24.8	0	na
	σ_{prop} (%)	3.57	20.8	14.4	20.1
	σ_{add} (mL/min)	4.83	12.1	17.7	8.57
Inter-individual variability	ω_{Kge} (%)	60.6	25.0	27.5	23.1
	ω_{Kse} (%)	18.6	0	21.6	0

RSE: relative standard error, standard error of estimate/estimate*100(%); na: not available

Final model evaluation

The individual predictions (IPRED) are generated by assuming new observations based on the individual parameter estimates of chosen individuals in the population, while the population predictions (PRED) are targeted to predict new observations of new individuals based on the estimated population means and residual error distributions. As shown in the A and B plots of Fig. 5, the dots scatter evenly along the two sides of the red line y=x when comparing the predicted and observed fluid volume in the stomach, indicating a good prediction quality. We also investigated on pattern of the weighted residual errors (WRES) and found it almost did not change much as PRED and time. This means that the WRES could be approximated with white noise. Therefore, the final model was demonstrated to be well developed.

Virtual predictive check (VPC) plots of gastric fluid volume profiles were shown in Fig. 6. Both 95% prediction intervals of the 500 simulated profiles based on ODE and SDE models with the incorporation of measurement errors covered most of the observations, with slightly more coverage provided by SDE. The greater interval areas in the SDE plot indicated the SDE model was a better fit for high variability than the ODE model. In the ODE plot, many observations lied outside of the 95% prediction interval in the absence of measurement error components, while those were well captured in the presence of measurement errors. This aligned with the previous statement about the limitation of ODE that all the IAV would be assigned to the measurement errors. When comparing simulations with and without the incorporation of measurement errors in the SDE group, a large overlap was observed, implying most of the IAV could be explained by the fluctuations of Kge.

Discussion

The transit in the upper GI tract of human is typically regarded as a continuous first-order process. However, an increasing amount of research demonstrated this process to be far from that simple. For liquid volumes of 240 to 800 mL, experimental measurements of GE half-time varied from 8 to 18 minutes[2-6]. In the fasted state, GE rate of liquid was shown to heavily rely on MMC phases and the larger volume of 200 mL phenol red solution was reported to leave the stomach with a half-life of 11.8 min, being less dependent on gastric motility than the smaller volume of 50 ml solution[6]. In the study of Mudie et al., 75% of the subjects displayed first-order emptying patterns while 25% had non-first order, biphasic emptying after drinking 240 mL water[7]. There is very limited published experimental evidence pertaining to intestinal transit rate in the fasted state. But according to the results of mass transport analysis of phenol red, a first-order process is obviously inadequate to characterize duodenal and jejunal transit[12]. Considering the high frequency of MMC in this region, MMC presumably plays a critical role in the complex hydrodynamics pattern in proximal small intestine.

GE and intestinal transit are more likely to occur in a discontinuous fashion inferred from experimental evidence and GI physiology theory. After Schiller et al. reported that that fluid in the fasted small intestine is not a continuous watery compartment but instead in discrete pockets of varying volumes, Mudie et al. further quantified the volume and number of water pockets in the small intestine of fasted healthy humans.[7, 13] The resting small bowel water was distributed in 8 ± 1 pockets of 4 ± 1 mL on average each, rose to 15 ± 1 pockets of 6 ± 2 mL each at peak time, and 16 ± 3 pockets of 5 ± 1 mL each at 45 min before gradually returning to the baseline level. Regardless of water intake, the number of liquid pockets in the smaller 0.5-2.5 mL size bin was markedly higher than all the larger bin sizes and that there was no significant difference between the remaining larger bin sizes, but most of the total volume of liquid was found in the larger pockets. At the time point of 45 min after water administration, the smallest pockets (0.5-2.5 mL) accounted for less than 5% of the total liquid volume, the smaller pockets (2.5-20 mL) claimed about 40% of the total volume, and the largest amount of liquid (~60% of the volume) was contained in a small number of large pockets (> 20 mL)[7]. To our knowledge of GI physiology, it is natural to relate the discrete fluid pockets with time-varying volumes phenomena 1) to the varying onset, frequency, amplitude, duration, direction and distance of antral contraction and small intestinal peristalsis, 2) to the phasic secretion of the stomach, pancreas, biliary system and intestinal mucosal, 3) and to the different frequency and extent of opening of pylorus and Sphicter of Oddi during MMC cycle. The above factors altogether make any attempts at building detailed mechanistic model of this process extremely difficult.

The identification of MMC-driven discontinuous, small volume of fluid pockets helps to explain the variability of oral drug absorption and consequently has significant implications for therapeutic drug monitoring, formulation selection and the design of clinical trials and BE studies. To begin with, the randomness of the dosing time relative to MMC phases undoubtably brings in the variation of the delivery of drug to the absorptive site. If the drug is administered at the beginning of MMC phase 1, then it will likely be kept in the stomach for a significant period of time by the pylorus; To the contrary, if the drug is dosed during phase 3, the strong contractile period, then it will pass the stomach through the fully open pylorus into the small intestine without residence. In this case, the absorption profiles would be quite variable due to distinct GI motility patterns. Relevant GI physiology, experimental observations, and pulished models with the assumption of random dosing time relative to MMC phases have been elaborated previously.[6, 8, 14-16] In

addition, the presence of the small fluid pockets would contribute to the within-subject variability of drug Cmax and Tmax. If the volume of a fluid pocket is lower than the volume needed to completely dissolve the drug particles it encloses, the undissolved drug will not be transported across the GI mucosal cells and show up in the circulating system together with the dissolved counterpart. These drug particles are often held back in the GI lumen until they encounter appropriate fluid pockets. For instance, in a study of Schiller et al, only 50% of the ingested non-disintegrating capsules were surrounded by fluid in the fasted small intestine[13]. Hence, the randomness of the timing and the size of fluid pockets drug particles exposed to may lead to the variation of the systemic appearance of low solubility drugs, especially in terms of Cmax and Tmax. Furthermore, the discontinuity of the fluid pocket would inevitably incur higher variability than a continuous fluid flow system. If a drug product is completely dissolved in the stomach, it will remain there until the arrival of the next antral contraction; If a drug product is emptied from the stomach as the undissolved particles, none of them will be dissolved in quiescent period before the next wave of intestinal peristalsis brings fluid pockets. So we speculate there are jumps in the cumulative plot of dissolved drug vs time. Collectively, huge IAV would be anticipated in the dissolution and systemic appearance profiles due to this super dynamic GI transit feature.

To our knowledge, this is the first study focusing on characterizing oral absorption related process using SDE-based mixed effects models. There have been some published applications of SDE-based mixed effects models in PK and PK/pharmacodynamics (PD)[11, 17, 18], but none of them centered on oral absorption. For stochastic oral absorption models, Talattof et al simulated the discontinuousness of fluid pockets in the fasted state with a nonhomogeneous Poisson process[19], but the discrete state space Poisson process compounded with a complex fluid pocket volume function is difficult to implement directly as a structural model of mixed effect models in any modeling software. Yokrattanasak et al developed a simple simulation model for GE in the fed state by Weiner process[20], but there is no corresponding SDE-based mixed effects model in the fed state reported to date.

Compared with the traditional first-order approximation with constant coefficient, an extension of the mixed effects modeling approach to incorporate SDE adequately described the highly dynamic gastric fluid volume system in fasted healthy subjects. It supported estimation and understanding the variable GE process. The large volume of fluid pockets emptied from the stomach could be approximated by a large Kge relative to the typical individual mean level. On the contrary, a very small Kge relative to the typical individual mean was used to represent a very sparse distribution along the proximal small intestine of small fluid pockets emptied from the stomach. The absolute maximum of $\sigma_{wKge}dW_i(t)$, that is, the largest fluctuation of Kge was expected in the transition from Phase 3 to Phase 1 of MMC. The SDE-based mixed effects model described the gastric fluid volume system with time-varying Kge using a modeling approach, and was used mainly for a diagnostic purpose in this study, that is, to find out the main driver of the system dynamics. More validations based on different external data are required to make it qualified as a simulation model with reliable predictive capacity.

As the gastric fluid volume only reflects a part of the hydrodynamics of the GI tract, future studies could potentially further explore the quantification of the fluid volume in other parts of the gut. For instance, developing a model simultaneously characterizing the fluid volume profiles in the stomach, duodenum, and jejunum would be important. Moreover, modeling the whole highly

variable oral drug absorption process in the SDE framework would be an interesting extension. For a deterministic (less dynamic) system, the trajectory can be adequately characterized using ODE. SDE has the advantage over ODE of modeling for a dynamic system because the stochastic component of SDE model can accommodate such dynamics to separate system dynamics from IAV. In this case, the dynamic GI transit and luminal pH fluctuations, etc., can be the main contributors to the GI dynamics.

It should be noted that the application of the EKF algorithm in this study assumed the random deviations of logKge from its typical individual mean could be sufficiently captured by a Gaussian distribution, that is a standard Wiener Process. Nevertheless, EKF cannot adequately approximate skewed or multimodal distributions. When the dynamics become more complex along the gut, such as in the duodenum, one could consider nonlinear estimators like particle filters.[18, 21, 22] Another caveat is that the periodic non-homogeneous motility patterns with different time intervals of MMC phases in the fasted state makes the fluctuations of logKge beyond just a standard Weiner Process. Alternatively, the employment of time-varying covariates such as the GI motility data measured by GI multi-lumen catheter[23] or SmartPill[24] to assist with describing Kge can be a promising, GI physiologically realistic strategy for this complex dynamic system.

Conclusion

The SDE-based mixed effects model developed from our study successfully characterized the gastric fluid volume profiles among the healthy subjects and provided a robust approximation of the physiological parameters in the very dynamic system. The remarkable IAV could be further separated into system dynamics terms and measurement error terms in the SDE model rather than empirically assigning all the IAV to measurement error in the traditional ODE method. The system dynamics were best captured by the random fluctuations of the gastric emptying coefficient Kge, indicating a mechanistic model with GI motility as a time-varying covariate of Kge is preferred in the future.

Acknowledgements

Main results were simply put together in the appendix of the PhD thesis of Kai Wang entitled with “Mechanistic Model-based Drug Oral Absorption Analysis”. Additional analysis and discussion were included in this manuscript.

Funding statement

This research received no specific grant from any funding agency in the public, commercial, or not-for-profit sectors.

Conflict of Interest

Nothing to declare.

Author contributions

Dr. Wang conducted the data analysis and drafted the manuscript. Dr. Marciani provided data. Dr. Marciani, Dr. Amidon, Dr. Smith, and Dr. Sun revised the manuscript. All authors approved the final version of the manuscript.

References

1. Hens B, Corsetti M, Spiller R, Marciani L, Vanuytsel T, Tack J, et al. Exploring gastrointestinal variables affecting drug and formulation behavior: Methodologies, challenges and opportunities. Int J Pharm. 2017;519(1-2):79-97. doi: 10.1016/j.ijpharm.2016.11.063.
2. Steingoetter A, Fox M, Treier R, Weishaupt D, Marincek B, Boesiger P, et al. Effects of posture on the physiology of gastric emptying: a magnetic resonance imaging study. Scand J Gastroenterol. 2006;41(10):1155-64. doi: 10.1080/00365520600610451.
3. Ramsbottom N, Knox MT, Hunt JN. Gastric-Emptying of Barium-Sulfate Suspension Compared with That of Water. Gut. 1977;18(7):541-2. doi: DOI 10.1136/gut.18.7.541.
4. Umenai T, Arai N, Chihara E. Effect of the preliminary hydration on gastric emptying time for water in healthy volunteers. Acta Anaesthesiol Scand. 2009;53(2):223-6. doi: 10.1111/j.1399-6576.2008.01832.x.
5. Wright J, Adams V, Hykin J, Gowland P, Issa B, Boulby P, et al. The measurement of gastric motor function and transit in man by echo planar magnetic resonance imaging. Magn Reson Mater Phy. 1994;2(3):467-9. doi: Doi 10.1007/Bf01705299.
6. Oberle RL, Chen TS, Lloyd C, Barnett JL, Owyang C, Meyer J, et al. The influence of the interdigestive migrating myoelectric complex on the gastric emptying of liquids. Gastroenterology. 1990;99(5):1275-82.
7. Mudie DM, Murray K, Hoad CL, Pritchard SE, Garnett MC, Amidon GL, et al. Quantification of gastrointestinal liquid volumes and distribution following a 240 mL dose of water in the fasted state. Mol Pharm. 2014;11(9):3039-47. doi: 10.1021/mp500210c.
8. Barrett KE. Gastrointestinal physiology. 2nd ed. McGraw-Hill's AccessMedicine. New York, N.Y.: McGraw-Hill Education LLC,; 2014.
9. DiMagno EP. Regulation of interdigestive gastrointestinal motility and secretion. Digestion. 1997;58 Suppl 1:53-5.
10. Kristensen NR, Madsen H, Jorgensen SB. Parameter estimation in stochastic grey-box models. Automatica. 2004;40(2):225-37. doi: 10.1016/j.automatica.2003.10.001.
11. Tornoe CW, Overgaard RV, Agerso H, Nielsen HA, Madsen H, Jonsson EN. Stochastic differential equations in NONMEM: implementation, application, and comparison with ordinary differential equations. Pharm Res. 2005;22(8):1247-58. doi: 10.1007/s11095-005-5269-5.
12. Paixao P, Bermejo M, Hens B, Tsume Y, Dickens J, Shedden K, et al. Gastric emptying and intestinal appearance of nonabsorbable drugs phenol red and paromomycin in human subjects: A multi-compartment stomach approach. Eur J Pharm Biopharm. 2018;129:162-74. doi: 10.1016/j.ejpb.2018.05.033.
13. Schiller C, Frohlich CP, Giessmann T, Siegmund W, Monnikes H, Hosten N, et al. Intestinal fluid volumes and transit of dosage forms as assessed by magnetic resonance imaging. Aliment Pharm Therap. 2005;22(10):971-9. doi: 10.1111/j.1365-2036.2005.02683.x.
14. Wang K, Li Y, Chen B, Chen H, Smith DE, Sun D, et al. In Vitro Predictive Dissolution Test Should Be Developed and Recommended as a Bioequivalence Standard for the Immediate-Release Solid Oral Dosage Forms of the Highly Variable Mycophenolate Mofetil. Mol Pharm. 2022;19(7):2048-60. doi: 10.1021/acs.molpharmaceut.1c00792.
15. Oberle RL, Amidon GL. The influence of variable gastric emptying and intestinal transit rates on the plasma level curve of cimetidine; an explanation for the double peak phenomenon. J Pharmacokinet Biopharm. 1987;15(5):529-44. doi: 10.1007/BF01061761.

16. Talattof A, Price JC, Amidon GL. Gastrointestinal Motility Variation and Implications for Plasma Level Variation: Oral Drug Products. Mol Pharmaceut. 2016;13(2):557-67. doi: 10.1021/acs.molpharmaceut.5b00774.
17. Leander J, Almquist J, Ahlstrom C, Gabrielsson J, Jirstrand M. Mixed Effects Modeling Using Stochastic Differential Equations: Illustrated by Pharmacokinetic Data of Nicotinic Acid in Obese Zucker Rats. AAPS J. 2015;17(3):586-96. doi: 10.1208/s12248-015-9718-8.
18. Krengel A, Hauth J, Taskinen MR, Adiels M, Jirstrand M. A continuous-time adaptive particle filter for estimations under measurement time uncertainties with an application to a plasma-leucine mixed effects model. BMC Syst Biol. 2013;7:8. doi: 10.1186/1752-0509-7-8.
19. Talattof A, Amidon GL. Pulse Packet Stochastic Model for Gastric Emptying in the Fasted State: A Physiological Approach. Mol Pharmaceut. 2018;15(6):2107-15. doi: 10.1021/acs.molpharmaceut.7b01077.
20. Yokrattanasak J, De Gaetano A, Panunzi S, Satiracoo P, Lawton WM, Lenbury Y. A Simple, Realistic Stochastic Model of Gastric Emptying. PLoS One. 2016;11(4):e0153297. doi: 10.1371/journal.pone.0153297.
21. Samuel Wiqvist AG, Ashleigh T. McLean, Umberto Picchini. Efficient inference for stochastic differential equation mixed-effects models using correlated particle pseudo-marginal algorithms. Computational Statistics & Data Analysis. 2021;157(107151). doi: https://doi.org/10.1016/j.csda.2020.107151.
22. Botha I, Kohn R, Drovandi C. Particle Methods for Stochastic Differential Equation Mixed Effects Models. Bayesian Analysis. 2021;16(2):575-609, 35.
23. Koenigsknecht MJ, Baker JR, Wen B, Frances A, Zhang H, Yu A, et al. In Vivo Dissolution and Systemic Absorption of Immediate Release Ibuprofen in Human Gastrointestinal Tract under Fed and Fasted Conditions. Mol Pharm. 2017;14(12):4295-304. doi: 10.1021/acs.molpharmaceut.7b00425.
24. Mikolajczyk AE, Watson S, Surma BL, Rubin DT. Assessment of Tandem Measurements of pH and Total Gut Transit Time in Healthy Volunteers. Clin Transl Gastroenterol. 2015;6:e100. doi: 10.1038/ctg.2015.22.

Figure legends

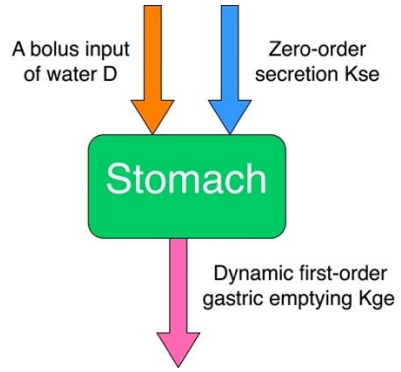

Fig. 1 Schematic illustration of the structural model for fluid volume in the stomach compartment. Kse and Kge are the coefficients for zero-order saliva and gastric secretion and first-order GE, respectively. D is the input function of water administration.

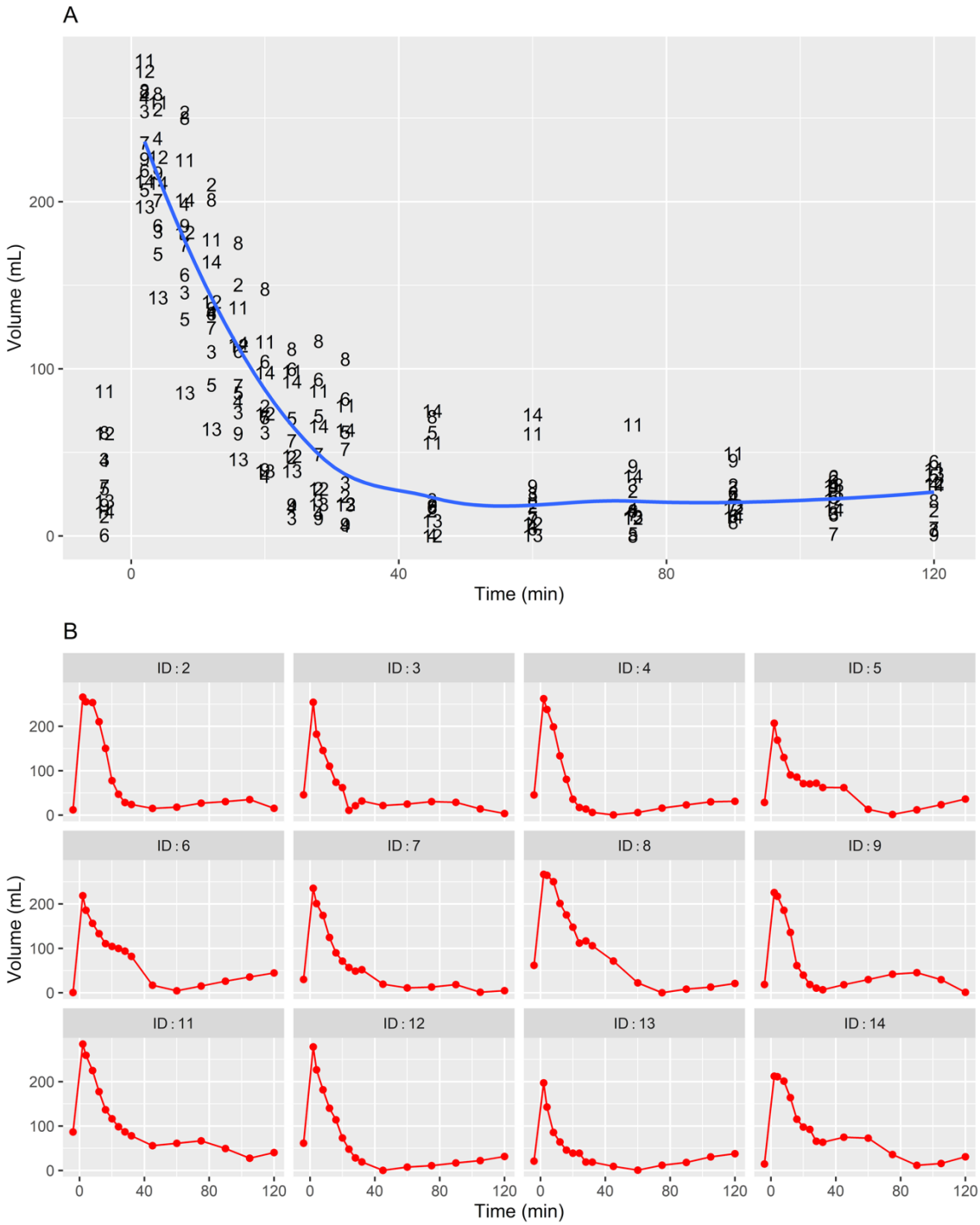

Fig. 2 Great IIV and IAV were shown in the overall observed gastric fluid volume profiles (A) and individual observed gastric fluid volume profiles (B), respectively. The blue curve in A is the locally weighted smoothing line among different subjects in the time course and the scattered numbers represent the identification number of each subject.

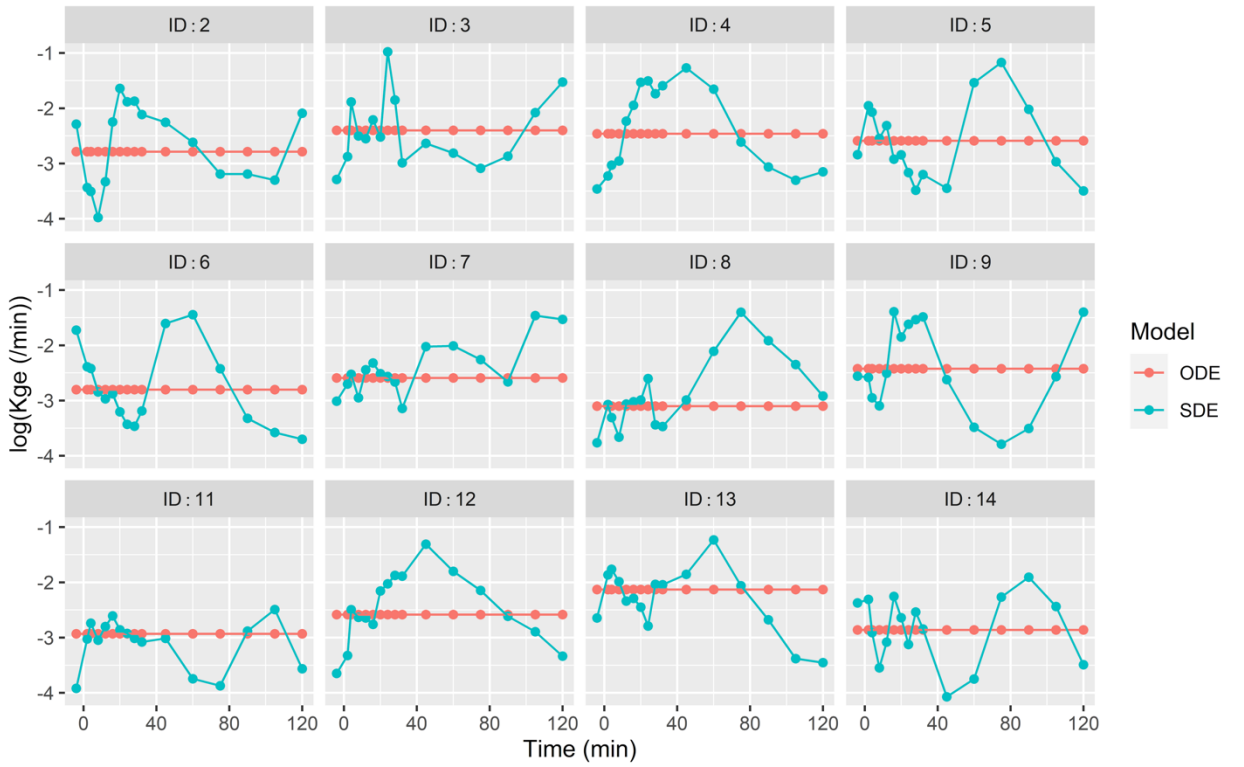

Fig. 3 Logarithm of Kge at each measurement for each individual via ODE and SDE, respectively.

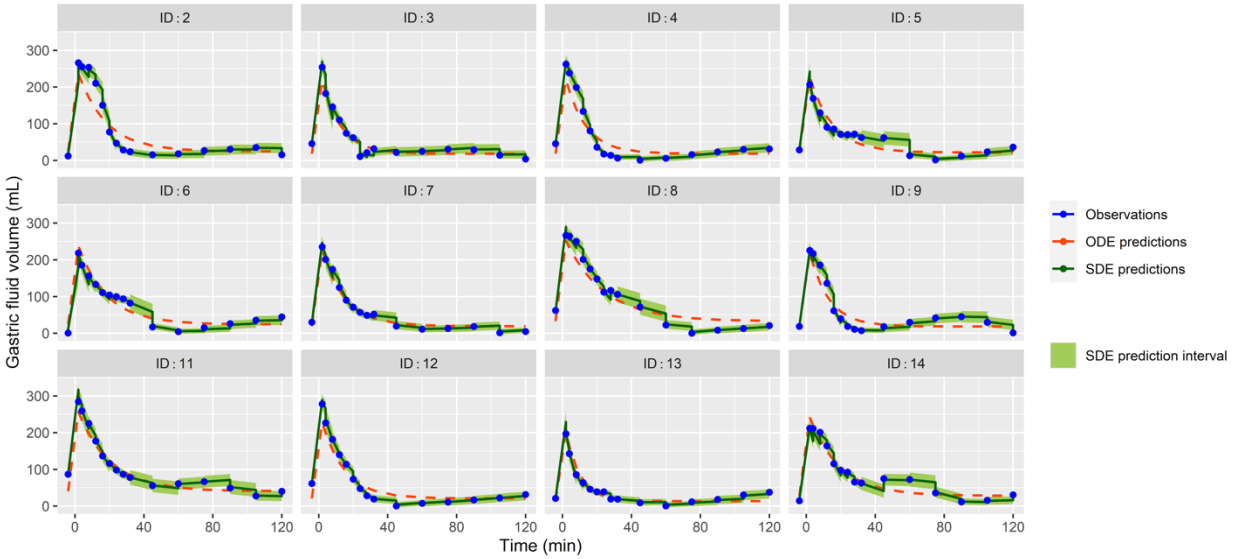

Fig. 4 Individual plots of the one-step SDE predictions, updates, and prediction interval plotted together with the ODE predictions. The SDE prediction interval is calculated by $\hat{y}_{j|j-1} \pm \sqrt{R_{j|j-1}}$.

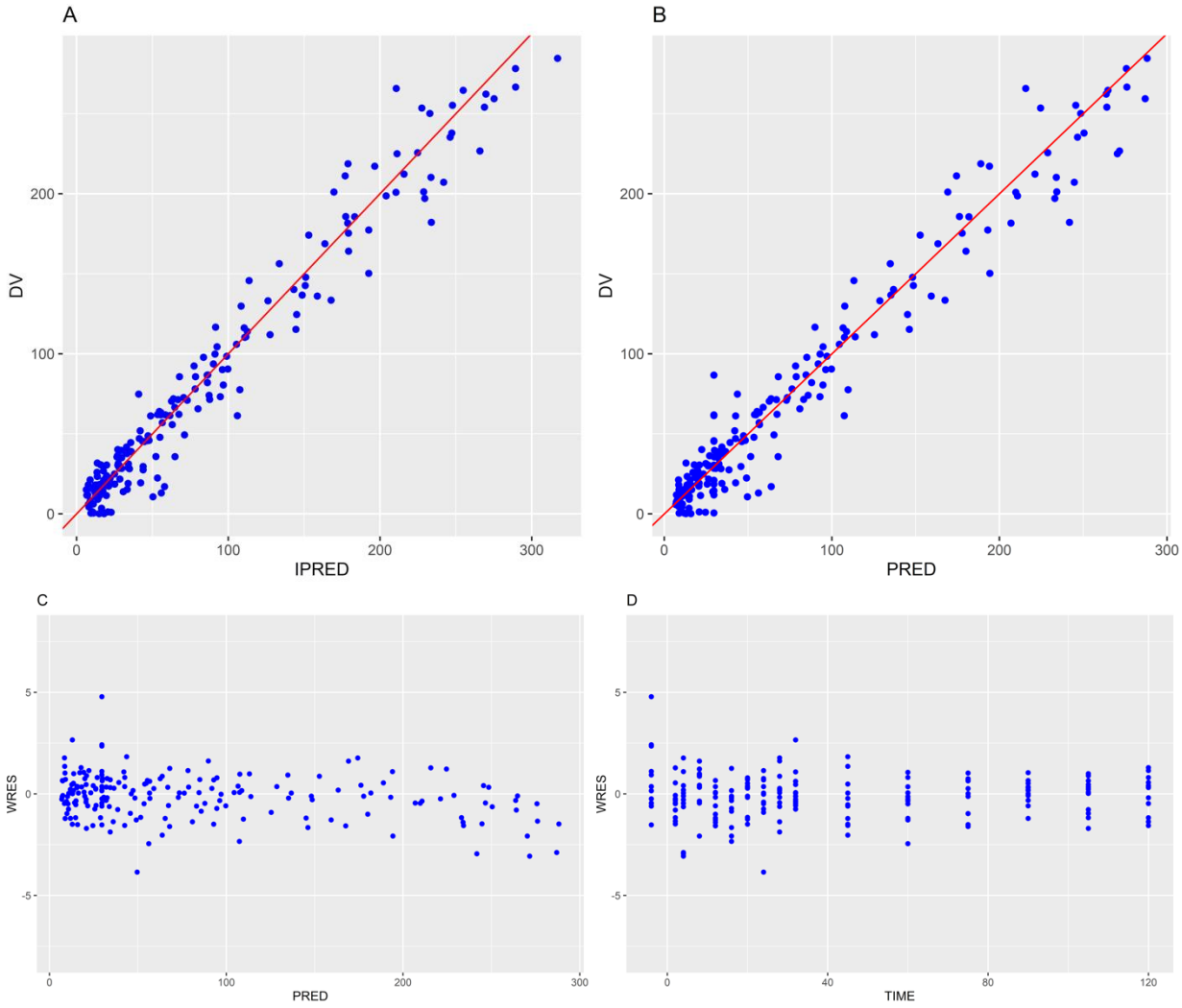

Fig. 5 Goodness-of-fit plots (A-D) of the SDE with time-varying Kge mixed effects model of the gastric fluid volume profiles among healthy subjects with EKF estimation algorithm. DV: observed gastric fluid volume (mL). IPRED: individual predictions of gastric fluid volume (mL); PRED: population predictions of gastric fluid volume (mL); WRES: weighted residual errors. TIME: minutes relative to the time of administering 240 mL of water.

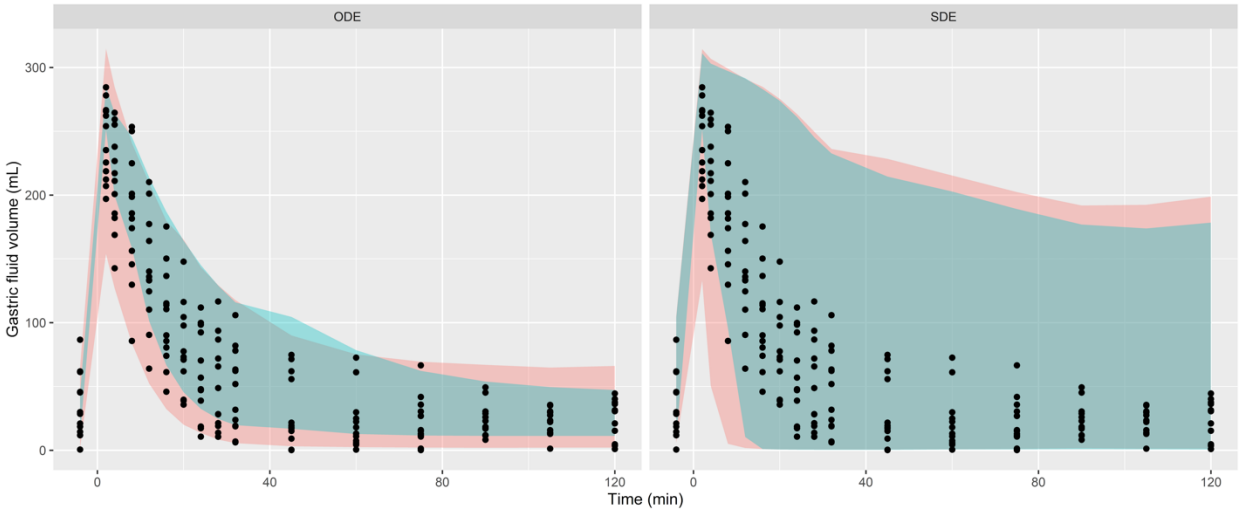

Fig. 6 VPC plots of gastric fluid volume profiles based on the ODE (left panel) and SDE (right panel) models, respectively. The green and red areas represent the 95% prediction intervals with and without the incorporation of the measurement errors, respectively. The black points are the observations of this study.